Vol. 16, No. 1, 2025
ISSN 2233-4203/ e-ISSN 2093-8950
ARTICLE www.msletters.org | Mass Spectrometry Letters

Quantitation of Peptides on Multiple Surfaces for Matrix-Assisted Laser Desorption/Ionization Fourier Transform Ion Cyclotron Resonance Mass Spectrometry: Comparison of Magnitude versus Absorption Modes

Alexandra M. Izydorczak[1], Kayla E. Mascaro[1], Kevin J. Zemaitis[1,2], and Troy D. Wood[1]*

[1]*Department of Chemistry, University at Buffalo, Buffalo, NY,USA*
[2]*Pacific Northwest National Laboratory, Richland, WA, USA*

Received September 4, 2024, Revised October 3, 2024, Accepted November 1, 2024
First published on the web March 31, 2025; DOI: 10.5478/MSL.2025.16.1.7

Abstract : Neuropeptides, particularly in tissues, can be difficult to detect due to their low amounts and similar structures to precursors. With matrix-assisted laser desorption/ionization mass spectrometry (MALDI MS), conventional organic acid matrices are used to help ionize analytes but can cause matrix interference in the *m/z* range of common neuropeptides. The high-resolution of Fourier transform ion cyclotron resonance mass spectrometry (FTICR MS) enables distinguishing matrix-derived signals from those of neuropeptides. Another benefit to FTICR MS is the ability to process transients in multiple modes, magnitude-mode and absorption-mode. Using the dried droplet method, leucine enkephalin (LE) samples containing gluten exorphin B5 (B5) internal standard were deposited onto surfaces with a siloxane grid; a stainless-steel target plate (SUS), indium-tin oxide (ITO) slide, and glass slides were used. To improve the crystallization of CHCA, freeze drying was employed. Calibration curves of LE had an R^2 of 0.88 to 0.93 when processed in magnitude-mode or post-processed in absorption-mode when spotted on SUS, ITO slides, or glass slides. Slopes were nearly equal whether processed in absorption- or magnitude mode and did not impact the limit of detection. However, the nature of substrate impacted calibration curve slopes, with ITO slides providing the steepest slope, followed by non-conductive glass, with stainless steel exhibiting the shallowest slopes and sensitivity. Peak shape was improved in absorption-mode (2.5-2.6x improvement of resolution and 1.9-2.9x improvement of S/N), suggesting that absorption-mode processing should be employed in quantitative FTICR MS applications.

Keywords : MALDI, FTICR MS, quantitation, Magnitude-mode, Absorption-Mode

Introduction

Neuropeptides are a diverse type of biomolecule used in the central peripheral nervous system for signaling in order to control and regulate essential physiological functions.[1-3] The most common approach to detect neuropeptides is immunohistochemistry (IHC); other techniques for identifying neuropeptides include high-performance liquid chromatography (HPLC), often coupled to mass spectrometry (MS), or Edman degradation.[2,4] These techniques have difficulties with detecting and identifying these peptides due to their low abundance. An alternative approach uses matrix-assisted laser desorption/ionization mass spectrometry (MALDI MS).[1] MALDI MS allows for intact molecular ions to be ionized due to its high sensitivity.[1] Leucine enkephalin (LE) is a pentapeptide made up of tyrosine, glycine, glycine, phenylalanine, and leucine (YGGFL) and is an endogenous brain pentapeptide that has opiate-like activites.[5] LE has been studied in mass spectrometry and has a $(M+H)^+$ of 556.2771 Da.[6] Gluten exorphin B5 (B5) is a pentapeptide that is made up of tyrosine, glycine, glycine, tryptophan, and leucine (YGGWL).[7] B5 also has opiate-like activity that comes from food, hence termed an exorphin as opposed to an endorphin.[7]

Fourier transform ion cylcotron resonance mass spectrometry (FTICR MS) has been around since its creation in 1974 by Comisarow and Marshall, and is reknowned for its high-resolution attributes.[8-10] FTICR is compatible with a MALDI source.[8,11] Modern FTICR MS shows resolving power up to 12 million when attached to a 21 Tesla (T) magnet, and increases in primary performance indicators such as sensitivity, resolving power, and dynamic range are also the result of higher magnetic field strength.[8,12,13] FTICR MS data can be processed in either

*Reprint requests to Troy D. Wood
https://orcid.org/0000-0002-2556-8511
E-mail: twood@buffalo.edu

magnitude-mode or absorption-mode.[14] The only way to extract absorption-mode data is to properly align the intial phase angles to correct for the real part of magnitude-mode data.[14-30] Proper phasing was an obstacle to FTICR MS until phasing solutions unlocked access to data in the absorption-mode.[21, 23] The calculated phase correction can then be broadly applied to individual or batches of acquired transients in a variety of manners.[16,31-33] The optimized phase correction function has been determined by an iterative or genetic algorithm, manual or automated approaches, or a specific spectrum is used to optimize for a similar spectrum.[16,18,21] Absorption-mode has shown both a larger number as well as narrower peaks than magnitude-mode allowing for an improvement of mass resolving power by at least 2 times and an increase in signal-to-noise ratio (S/N) by at least $\sqrt{2}$.[14-23,29] Experimental confirmation after absorption-mode processing is necessary for two reasons. Magnitude-mode data includes dispersion-mode data, which inherently broadens the peak shape. Also, for multiple species, the absorption-mode data is the sum of all components; even if the absorption-mode data is correctly phased, the dispersion-mode spectra of two closely-spaced peaks can partly cancel. Thus, Marshall and Verdun concluded that magnitude-mode processing is unsuitable for the purposes of quantitative analysis.[28]

MALDI was created in the late 1980s by Karas and Hillenkamp for organic matrices and by Tanaka with cobalt nanoparticles.[8,34-36] MALDI is capable of analyzing various types of compounds at the same time, being easy to operate, with high accuracy and reproduciblity, high speed, sensitive detection, little sample consumption, and a high salt tolerance.[37,38] MALDI is able to detect molecules with *m/z* from hundreds of Da to MDa.[37,39-48] This is a very common technique involving a specific set of sample preparation procedures. The most common approaches of sample application include dried droplet and sublimation.[8] The target plates typically used are conductive including stainless-steel, standard nickel-coated aluminum, or indium-tin oxide (ITO) slides.[8] There is some interest in using non-conductive surfaces that use a conductive coating like gold or resins.[49] Here, quantitative MALDI FTICR MS is evaluated using different substrates by both absorption-mode and magnitude-mode processing.

Experimental

Chemicals

Matrix used was 97% grade CHCA from Sigma Aldrich (St. Louis, MO, USA). Analytes for quantiation were B5 from BACHEM AG (Bubendorf, Switzerland) and LE from American Peptide (Sunnyvale, CA, USA). The solvents used to make solutions were HPLC grade methanol (MeOH) from Sigma Aldrich (St. Lousi, MO, USA), acetonitrile (ACN) from Thermo Scientific (Bellefonte, PA, USA), water from Thermo Scientific (Bellefonte, PA, USA), formic acid (FA) from Fisher Scientific (Fair Lawn, NJ, USA), and trifluoroacetic acid (TFA) from EMD Chemicals (Gibbstown, NJ, USA). Siloxane mixture was made with poly (dimethyl siloxane) vinyl terminated (PDMS-vinyl terminated) from Aldrich Chemical (Milwaukee, WI, USA) and hexanes from Fisher Scientific (Hampton, NH, USA). Glycerol was from Acros Organics (Geel, Antwerp, Belgium). Sodium hydroxide (NaOH) was used from J.T. Baker (Phillipsburg, NJ, USA).

Methods

For the dried droplet method a siloxane grid was formed on SUS plates, ITO slides, and glass slides based on the method of Redeby et al.[50] A 5 g/L solution of PDMS-vinyl terminated is made by diluting a 5 mL of a 50 g/L PDMS-vinyl terminated solution to 50 mL with hexanes. Glycerol is spotted to the sample surfaces with a 0.1-10 μL pipette tip on predetermined spots. Then the siloxane mixture is sprayed onto each surface with a Paasche airbrush to cover evenly with about 15 passes. The siloxane film was dried in an oven at 75°C for 5 minutes. Once the film is dry the glycerol is removed with DI water.

Samples were made by dissolving LE in ACN with concentrations of 100, 200, 300, 400, 500, 650, 750, 850, and 1000 ppb. B5 was made by dissolving in ACN at 1000 ppb. The optimized matrix was 20 mg/mL CHCA in 90:10:0.1 ACN:H_2O:TFA. The sample mixture used for dried droplet was 25 μL of the concentration desired of LE solution, 25 μL of 1000 ppb B5 solution, 25 μL of CHCA solution, 20 μL of a 10% FA solution, and 5 μL ACN. Once the grid was made on either SUS, ITO slide, or a glass slide, 1.0 μL of the sample mixture was deposited on the slides in the predetermined spots. Once the spots were applied they were dried with a X-Large pro freeze dryer from Harvest Right, the freeze time was 5 minutes, the dry time was 5 minutes, and the final dry time of 2 mintues.

All samples were analyzed with an unmodified commercial Bruker Daltonics 12 T SolariX FTICR MS equipped with an Infinity cell and MALDI source with a 1 kHz SmartBeam II frequency-tripled (355 nm) Nd:YAG laser (Bremen, Germany). Instrument parameters were optimized to include a broadband excitation with a 1 M time domain, and a *m/z* range of 147.43-1500.00 resulting in a transient of 0.4194 s. The number of acquisitions was 75, with a laser focus of small, a laser frequency of 1000 Hz, number of shots are 1000. Laser power was optimized on standards before MS acquisitions. The data was processed with DataAnalysis 5.0 (Bruker Daltonics, Bremen, Germany) and ftmsProcessing 2.2.0.

Samples were tuned with an external calibration of sodium trifluoroacetate (NaTFA). NaTFA was made with 0.1% TFA titrated with 10 mmol/L NaOH to a pH between 3 to 4, then diluted 50% with ACN.[51] The *m/z* scale was internally calibrated with CHCA adducts of $[2M+H]^+$, $[2M+Na]^+$, $[2M+K]^+$, and $[3M+H]^+$. Absorp-

tion-mode data was processed with 1 M data points zero-filled once, Kilgour window mode with a Kilgour Max of 0.5, advanced AMP Parameters of use genetic algorithm, AMP Baseline Correct of Simple_100, AMP *m/z* range of 200-1000, and finding a genetic algorithm score of ≥ 0.8 and < 1.0.

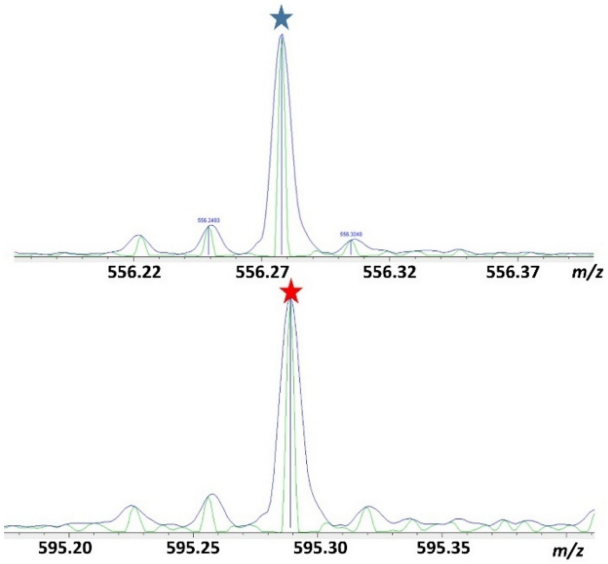

Figure 1. Spectra on SUS with LE $[M+H]^+$, marked with a blue star, on top and B5 $[M+H]^+$, marked with a red star, on bottom, where blue line represents magnitude-mode and green line represents absorption-mode.

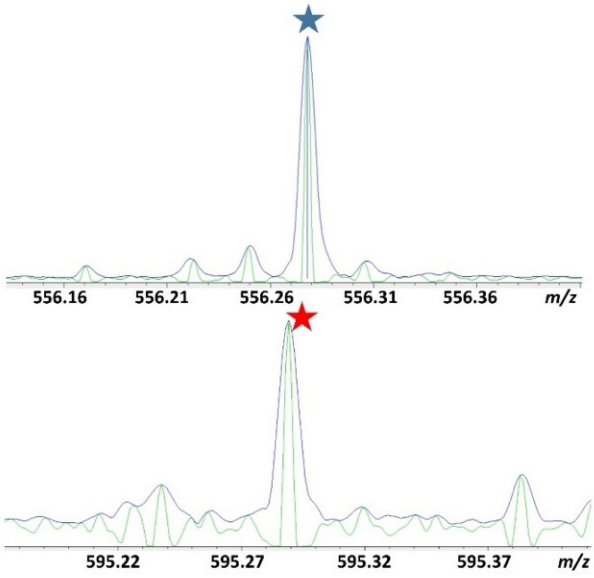

Figure 2. Spectra on ITO with LE $[M+H]^+$, marked with a blue star, on top and B5 $[M+H]^+$, marked with a red star, on bottom, where blue line represents magnitude-mode and green line represents absorption-mode.

Results

Calibration curves were constructed by plotting the concentration ratio of LE/B5 versus the LE/B5 $(M+H)^+$ peak intensity. The lower limit of detection on all the surfaces was 200 ppb LE (LE was undetected at 100 ppb). When comparing the peak shapes of magnitude-mode versus absorption-mode, the absorption-mode peaks had consistently higher resolving power, as demonstrated with the examples shown in Figures 1-3 and summarized in Table 1. When comparing the averaged resolving power from all

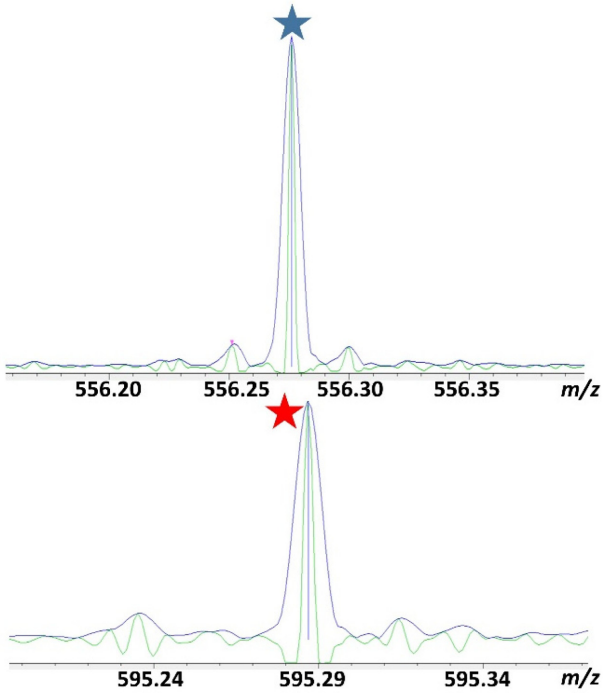

Figure 3. Spectra on glass with LE $[M+H]^+$, marked with a blue star, on top and B5 $[M+H]^+$, marked with a red star, on bottom, where blue line represents magnitude-mode and green line represents absorption-mode.

Table 1. Comparison of mean Signal-to-noise (S/N) and mean resolving power for $(M+H)^+$ peaks of leucine enkephalin (LE) and gluten exorphin B5 as a function of surface and processing mode; Abs = absorption-mode, Mag = magnitude-mode.

Mode	S/N LE	S/N B5	RP LE	RP B5
SUS (Abs)	1335	883	187826	177259
SUS (Mag)	705	307	74939	71244
ITO (Abs)	1012	378	184476	175269
ITO (Mag)	433	167	71250	70915
Glass (Abs)	635	251	190208	178500
Glass (Mag)	222	116	74996	71319

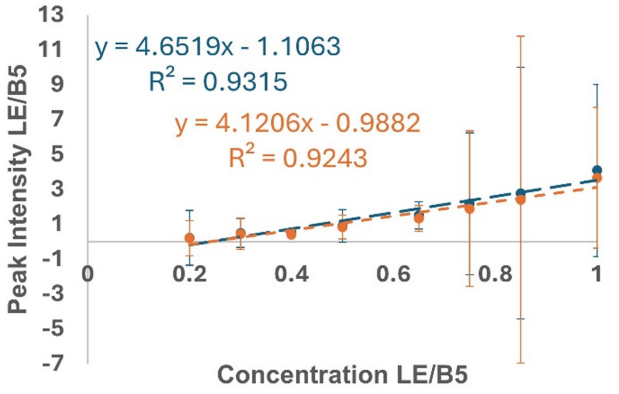

Figure 4. Calibration curve of overall average of peak intensity on SUS plate in magnitude-mode, blue, and absorption-mode, orange.

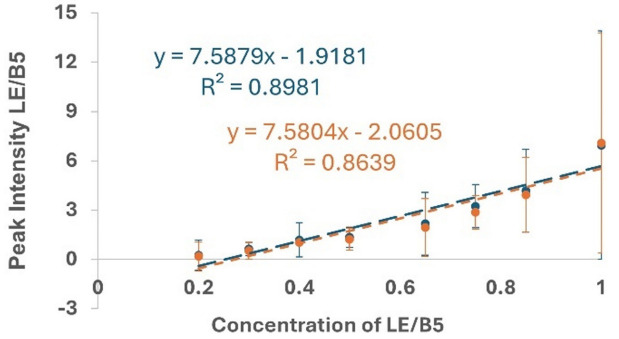

Figure 5. Calibration curve of overall average of peak intensity on ITO slide in magnitude-mode, blue, and absorption-mode, orange.

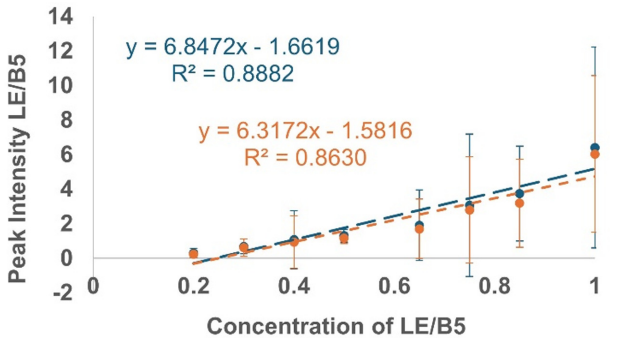

Figure 6. Calibration curve of overall average of peak intensity on glass plate in magnitude-mode, blue, and absorption-mode, orange.

surfaces, the absorption-mode observed resolution showed 2.5-2.6 times enhancement and the S/N was 1.9-2.9 times better. The calibration curves were linear for all surfaces. For SUS the R^2 for magnitude-mode was 0.9315, shown in Figure 4 in blue, and for absorption-mode was 0.9243, shown in Figure 4 in orange.

The calibration curve for ITO had R^2 of 0.8981 for magnitude-mode, in Figure 5 in blue, and 0.8639 for absorption-mode, in Figure 5 in orange. The calibration curve for ITO had R^2 of 0.8882 for magnitude-mode, in Figure 6 in blue, and 0.8630 for absorption-mode, in Figure 6 in orange.

Discussion

Absorption-mode processing improved the peak shape, resolution, and S/N by approximately a factor of 2 over magnitude-mode. This upholds the improvement in peak shape, resolution, and S/N as mentioned in theory for absorption-mode vs. magnitude-mode FTICR MS, and is demonstrated on multiple surface types using dried droplet MALDI method. There are no significant differences in linearity when using absorption-mode or magnitude-mode; linear curves with an R^2 of at least 0.8857 and up to 0.9337 on all surfaces, with a linear range of 200 ppb to 1000 ppb. Linear calibration curves on three surface types (where two are conductive and one is not) down to 200 ppb are demonstrated. The nature of the surface did not change the limit of detection, and slopes between absorption-mode and magnitude-mode processing are virtually equal. However, ITO surfaces exhibited the highest slope in terms of sensitivity, followed by non-conducting glass with stainless steel surfaces providing the shallowest slopes.

Conclusions

Absorption-mode post-processing was used for FTICR MS combined with MALDI and was able to show evidence of peak shape, resolution, and S/N improvement of at least two fold. MALDI was performed on SUS plate, ITO slide, and glass slide, creating calibration curves from dried droplet application from 200 ppb to 1000 ppb. Further research should examine other surfaces and other matrix types, for example two-dimensional graphene, to see if further linearity and/or lower detection limits can be achieved. Application of samples can also be further studied in order to improve linearity and limit of detection, and eventually application to the quantitation of neuropeptides in imaging approaches. Our results suggest that absorption-mode processing should become the mode of choice when processing quantitative FTICR MS data.

Acknowledgments

We gratefully acknowledge the NIH (Grant# S10-RRO29517-01) for support in acquiring a Bruker 12 T SolariX FT-ICR MS and the University at Buffalo Chemistry Instrument Center.

Conflicts of Interest

The authors declare no competing financial interest.

References

1. Zimmerman, T.A.; Rubakhin, S.S.; Romanova, E.V.; Tucker, K.R.; Sweedler, J.V. *Anal. Chem.* **2009**, 81, 9402. https://doi.org/10.1021/ac901820v
2. Ly, A.; Ragionieri, L.; Liessem, S.; Becker, M.; Deininger, S.-O.; Neupert, S.; Predel, R. *Anal. Chem.* **2019**, 91, 1980. https://doi.org/10.1021/acs.analchem.8b04304
3. Hulme, H.; Fridjonsdottir, E.; Gunnarsdottir, H.; Vallianatou, T.; Zhang, X.; Wadensten, H.; Shariatgorji, R.; Nilsson, A.; Bezard, E.; Svenningsson, P.; Andren, P.E. *Neurobiol. Dis.* **2020**, 137, 104738. https://doi.org/10.1016/j.nbd.2020.104738
4. Rubakhin, S.S.; Greenough, W.T.; Sweedler, J.V. *Anal. Chem.* **2003**, 75, 5374. https://doi.org/10.1021/ac034498+
5. Lukiw, W.J. *Cell. Mol. Neurobiol.* **2006**, 26, 1001. https://doi.org/10.1007/s10571-006-9100-6
6. Sztaray, J.; Memboeuf, A.; Drahos, L.; Vekey, K. *Mass Spectrom. Rev.* **2011**, 30, 298. https://doi.org/10.1002/mas.20279
7. Fanciulli, G.; Dettori, A.; Demontis, M.P.; Tomasi, P.A.; Anania, V.; Delitala, G. *Life Sci.* **2005**, 76, 1713. https://doi.org/https://doi.org/10.1016/j.lfs.2004.09.023
8. Poole, C.F. *Chromatographia* **2018**, 81, 365. https://doi.org/10.1007/s10337-017-3400-5
9. Comisarow, M.B.; Marshall, A.G. *J. Mass Spectrom.* **1996**, 31, 581. https://doi.org/10.1002/(SICI)1096-9888(199606)31:6<581::AID-JMS369>3.0.CO;2-1
10. Marshall, A.G.; Hendrickson, C.L.; Jackson, G.S. *Mass Spectrom. Rev.* **1998**, 17, 1. https://doi.org/10.1002/(SICI)1098-2787(1998)17:1<1::AID-MAS1>3.0.CO;2-K
11. Amstalden van Hove, E.R.; Smith, D.F.; Heeren, R.M.A. *J. Chromatogr. A* **2010**, 1217, 3946. https://doi.org/10.1016/j.chroma.2010.01.033
12. Hendrickson, C.L.; Quinn, J.P.; Kaiser, N.K.; Smith, D.F.; Blakney, G.T.; Chen, T.; Marshall, A.G.; Weisbrod, C.R.; Beu, S.C. *J. Am. Soc. Mass Spectrom.* **2015**, 26, 1626. https://doi.org/10.1007/s13361-015-1182-2
13. Shaw, J.B.; Lin, T.-Y.; Leach, F.E., III; Tolmachev, A.V.; Tolic, N.; Robinson, E.W.; Koppenaal, D.W.; Pasa-Tolic, L. *J. Am. Soc. Mass Spectrom.* **2016**, 27, 1929. https://doi.org/10.1007/s13361-016-1507-9
14. Vandergrift, G.W.; Kew, W.; Lukowski, J.K.; Bhattacharjee, A.; Liyu, A.V.; Shank, E.A.; Paša-Tolić, L.; Prabhakaran, V.; Anderton, C.R. *Anal. Chem.* **2022**, 94, 3629. https://doi.org/10.1021/acs.analchem.1c05216
15. Xian, F. Broadband phase correction of Fourier transform ion cyclotron resonance mass spectra, Ph.D. Dissertation, Florida State University, **2012**.
16. Qi, Y.; Barrow, M.P.; Li, H.; Meier, J.E.; Van Orden, S.L.; Thompson, C.J.; O'Connor, P.B. *Anal. Chem.* **2012**, 84, 2923. https://doi.org/10.1021/ac3000122
17. Bills, J.R.; Nagornov, K.O.; Kozhinov, A.N.; Williams, T.J.; Tsybin, Y.O.; Marcus, R.K. *J. Am. Soc. Mass Spectrom.* **2021**, 32, 1224. https://doi.org/10.1021/jasms.1c00051
18. Smith, D.F.; Kilgour, D.P.; Konijnenburg, M.; O'Connor, P.B.; Heeren, R.M. *Anal. Chem.* **2013**, 85, 11180. https://doi.org/10.1021/ac403039t
19. Kooijman, P.C.; Nagornov, K.O.; Kozhinov, A.N.; Kilgour, D.P.A.; Tsybin, Y.O.; Heeren, R.M.A.; Ellis, S.R. *Sci. Rep.* **2019**, 9, 1. https://doi.org/10.1038/s41598-018-36957-1
20. Grgic, A.; Nagornov, K.O.; Kozhinov, A.N.; Michael, J.A.; Anthony, I.G.; Tsybin, Y.O.; Heeren, R.M.; Ellis, S.R. *Anal. Chem.* **2024**, 96, 794. https://doi.org/10.1021/acs.analchem.3c04146
21. Qi, Y.; Thompson, C.J.; Van Orden, S.L.; O'connor, P.B. *J. Am. Soc. Mass Spectrom.* **2011**, 22, 138. https://doi.org/10.1007/s13361-010-0006-7
22. Qi, Y.; Barrow, M.P.; Van Orden, S.L.; Thompson, C.J.; Li, H.; Perez-Hurtado, P.; O'Connor, P.B. *Anal. Chem.* **2011**, 83, 8477. https://doi.org/10.1021/ac2017585
23. Xian, F.; Hendrickson, C.L.; Blakney, G.T.; Beu, S.C.; Marshall, A.G. *Anal. Chem.* **2010**, 82, 8807. https://doi.org/10.1021/ac101091w
24. Marshall, A.G. *J. Chem. Phys.* **1971**, 55, 1343. https://doi.org/10.1063/1.1676226
25. Comisarow, M.B. *J. Chem. Phys.* **1971**, 55, 205. https://doi.org/10.1063/1.1675510
26. Comisarow, M.B.; Marshall, A.G. *Can. J. Chem.* **1974**, 52, 1997. https://doi.org/10.1139/v74-28
27. Marshall, A.G.; Roe, D.C. *Anal. Chem.* **1978**, 50, 756. https://doi.org/10.1021/ac50027a023
28. Marshall, A.G.; Verdun, F.R. *Fourier transforms in NMR, optical, and mass spectrometry: a user's handbook*, Elsevier. Amsterdam, **2016**
29. Kilgour, D.P.; Wills, R.; Qi, Y.; O'Connor, P.B. *Anal. Chem.* **2013**, 85, 3903. https://doi.org/10.1021/ac303289c
30. Craig, E.C.; Marshall, A.G. *J. Mag. Res.* **1988**, 76, 458. https://doi.org/10.1016/0022-2364(88)90350-2
31. Craig, E.C.; Santos, I.; Marshall, A.G.; Nibbering, N. *Rapid Commun. Mass Spectrom.* **1987**, 1, 33. https://doi.org/10.1002/rcm.1290010209
32. De Graaf, R.A. *In vivo NMR Spectroscopy: Principles and Techniques*, John Wiley & Sons. Hoboken, NJ, **2019**
33. Ernst, R.R.; Bodenhausen, G.; Wokaun, A. *Principles of nuclear magnetic resonance in one and two dimensions*, Oxford University Press. New York, **1990**
34. Bahr, U.; Deppe, A.; Karas, M.; Hillenkamp, F.; Giessmann, U. *Anal. Chem.* **1992**, 64, 2866. https://doi.org/10.1021/ac00046a036
35. Karas, M.; Bachmann, D.; Bahr, U.; Hillenkamp, F. *Int. J. Mass Spectrom. Ion. Proc.* **1987**, 78, 53. https://doi.org/10.1016/0168-1176(87)87041-6.
36. Tanaka, K.; Waki, H.; Ido, Y.; Yoshida, Y.; Yoshida, T. *Rapid Commun. Mass Spectrom.* **1988**, 2, 151. https://doi.org/10.1002/rcm.1290020802
37. Norris, J.L.; Caprioli, R.M. *Chem. Rev.* **2013**, 113, 2309.

https://doi.org/10.1021/cr3004295
38. Zhu, Z.; Shen, J.; Xu, Y.; Guo, H.; Kang, D.; Yu, T.; Wang, H.; Xu, W.; Wang, G.; Liang, Y. *J. Mass Spectrom.* **2019**, 54, 684. https://doi.org/10.1002/jms.4385
39. Shi, C.; Meng, J.; Deng, C. *J. Mater. Chem.* **2012**, 22, 20778. https://doi.org/10.1039/c2jm34745h
40. Fang, X.; Zhang, K.; Yang, P.; Qiao, L.; Liu, B. *Rapid Commun. Mass Spectrom.* **2016**, 30, 128. https://doi.org/10.1002/rcm.7617
41. Sha, Y.; Huang, D.; Zheng, S.; Deng, C. *Anal. Methods* **2013**, 5, 4585. https://doi.org/10.1039/c3ay40931g
42. Wan, D.; Gao, M.; Wang, Y.; Zhang, P.; Zhang, X. *J. Sep. Sci.* **2013**, 36, 629. https://doi.org/10.1002/jssc.201200766
43. Liu, Y.; Liu, J.; Yin, P.; Gao, M.; Deng, C.; Zhang, X. *J. Mass Spectrom.* **2011**, 46, 804. https://doi.org/10.1002/jms.1952
44. Min, Q.; Zhang, X.; Chen, X.; Li, S.; Zhu, J.-J. *Anal. Chem.* **2014**, 86, 9122. https://doi.org/10.1021/ac501943n
45. Hayasaka, T.; Goto-Inoue, N.; Masaki, N.; Ikegami, K.; Setou, M. *Surf. Interface Anal.* **2014**, 46, 1219. https://doi.org/10.1002/sia.5592
46. Enthaler, B.; Bussmann, T.; Pruns, J.K.; Rapp, C.; Fischer, M.; Vietzke, J.-P. *Rapid Commun. Mass Spectrom.* **2013**, 27, 878. https://doi.org/10.1002/rcm.6513
47. Rao, Z.; Geng, F.; Zhou, Y.; Cao, D.; Kang, Y. *Anal. Methods* **2017**, 9, 2014. https://doi.org/10.1039/C7AY00112F
48. Wenzel, R.J.; Matter, U.; Schultheis, L.; Zenobi, R. *Analytical Chemistry* **2005**, 77, 4329. https://doi.org/10.1021/ac0482054
49. 2019. Mass spectrometry imaging on mixed conductive/non-conductive substrate using JMS-S3000 SpiralTOF™ JEOL Ltd
50. Redeby, T.; Roeraade, J.; Emmer, Å. *Rapid Commun. Mass Spectrom.* **2004**, 18, 1161. https://doi.org/10.1002/rcm.1466
51. Moini, M.; Jones, B.L.; Rogers, R.M.; Jiang, L. *J. Am. Soc. Mass Spectrom.* **1998**, 9, 977. https://doi.org/10.1016/S1044-0305(98)00079-8

